Author(s): Lehto, Pauli & Remes, Heikki & Saukkonen, Tapio & Hänninen, Hannu & Romanoff, Jani

Title: Influence of grain size distribution on the Hall Petch relationship of welded structural steel

Year: 2014

Version: Post print

Please cite the original version:

Lehto, Pauli & Remes, Heikki & Saukkonen, Tapio & Hänninen, Hannu & Romanoff, Jani. 2014. Influence of grain size distribution on the Hall Petch relationship of welded structural steel. Materials Science and Engineering: A. Volume 592. 28-39. ISSN 0921-5093 (printed). DOI: 10.1016/j.msea.2013.10.094.

Influence of grain size distribution on the Hall-Petch relationship of welded structural steel

Pauli Lehto [a,*], Heikki Remes [a], Tapio Saukkonen [b], Hannu Hänninen [b], Jani Romanoff [a]

[a] Department of Applied Mechanics, Aalto University, School of Engineering, P.O. BOX 15300, FIN-00076 Aalto, Finland

[b] Department of Engineering Design and Production, Aalto University, School of Engineering, P.O. BOX 14200, FIN-00076 Aalto, Finland

* Corresponding author at: Department of Applied Mechanics, Aalto University, School of Engineering, P.O. BOX 15300, FIN-00076 Aalto, Finland. Tel.: +358 505233544. E-mail address: pauli.lehto@aalto.fi (P. Lehto).

Abstract

The strength of polycrystalline metals increases with a decrease in grain size according to the Hall-Petch relationship. However, heterogeneous microstructures deviate from this relationship depending on the distribution of grain sizes. This paper introduces a rule of mixtures based approach for determining the characteristic length of the microstructure for heterogeneous weld metal. The proposed grain size parameter, the volume-weighted average grain size, is measured experimentally for nine structural steel weld metals and two base materials. The weld metals are found to have a large variety of grain size distributions that are noticeably broader than those of the base material due to differences in phase contents. The results show that the volume-weighted average grain size is able to capture the influence of grain size distribution on the strength of welded structural steel. Based on the experimental results, a modified Hall-Petch relationship is formulated for the strength prediction of heterogeneous microstructures. The modified relationship is also found to be applicable to data from the literature.

Keywords

Grain size, Hall-Petch relationship, Hardness, Strength, Steel, Welding

1 Introduction

New lightweight solutions are needed to improve the energy efficiency of steel structures. Further development of the steel structures requires the utilisation of new materials and advanced production technology. In this development work, one of the fundamental issues is to understand the relation between microstructural quantities and material properties. This is especially challenging for advanced joining methods such as laser welding, where the properties of the narrow joint differ significantly from those of the base material [1–5].

In general, the mechanical properties of metallic materials have shown to correlate with the microstructural dimensions, most commonly with the average grain size. Based on the work of Hall [6] and Petch [7], a relationship was found between grain size and the mechanical properties of steel. For yield strength the relationship is formulated:

$$\sigma = \sigma_0 + kd^{-1/2}, \tag{1}$$

where σ_0 is the lattice friction stress required to move individual dislocations, k is a material-dependent constant known as the Hall-Petch slope, and d is the average grain size [8]. The work of Hall and Petch was focused on the lower yield point and the cleavage fracture stress of mild steel, respectively. Since then, the Hall-Petch relationship has been applied to a large variety of materials and material properties, such as hardness, stress-strain properties and fatigue [9–15]. As the Hall-Petch relationship is related to the measure of grain size, the correct definition of the effective grain size is crucial. Typically the average grain size is used to describe the microstructure [16], but its suitability for heterogeneous microstructures is questionable. Several investigations [8,16–21] have shown that the grain size distribution has an effect on the mechanical properties. For example, Berbenni *et al.* [20] showed that for a given average grain size, broadening of the grain size dispersion reduces the strength of the material.

To consider the influence of grain size distribution, Kurzydlowski [22] proposed an alternative approach, where the strength of different grain sizes was estimated by applying a weighting factor equal to the volume of the grains. This approach was further developed by Raeisinia and Sinclair [23]. They proposed a new geometric grain size parameter, the representative grain size, which eliminates the influence of grain size distribution on the Hall-Petch relationship. The fundamental assumptions of this approach are that all grains have the same shape and that the grain size distribution is log-normal. The same assumptions have been used in various numerical simulations of fictitious grain size distributions [16,24–27]. However, the previous studies [8,16–21,24,27] are focused on single phase base materials and do not cover heterogeneous weld metals.

The objective is to study the grain size distribution of weld metals and its influence on the Hall-Petch relationship. Furthermore, methods for the characterization of the grain size distribution are extended to be applicable for weld metal microstructures. The microstructures of nine structural steel weld

metals and two base materials are characterised using electron backscatter diffraction (EBSD) and optical microscopy. Because of the narrow welds, micro-indentation is applied for mechanical testing. Based on the experimental results, a modified Hall-Petch relationship is introduced for the strength prediction of heterogeneous microstructures. The study utilises stereological methods for estimating the volume fraction of grains from their surface area fractions. The investigation is limited to the transverse cross-sections of the material and thus the effects caused by grain shape three-dimensionality are omitted.

2 Definitions

Based on the role of grain boundaries as an effective barrier to the movement of dislocations, the grain size dependence of yield strength can be explained by the pile-up of dislocations at grain boundaries [6]. The pile-up causes an additional stress, which allows the deformation to be transmitted to the next grain. The additional stress is in relation to the number of dislocations in a pile-up, which is limited by the length of the slip band that can be identified with the average grain diameter [6]. Other theories have also been proposed for the grain size dependence, such as the dislocation density model [28–30] and the geometrically necessary dislocation (GND) model [31–33]. A review of the models is given by Zhu *et al.* [34] and Evers *et al.* [35]. Each model implies a different Hall-Petch slope k, but the mechanical properties are always scaled with the average grain diameter [34]. The average grain diameter, or in most cases the average grain size, is obtained from the experimental measurements [16,24]. The average grain size is defined as:

$$d = \frac{1}{n}\sum_{i=1}^{n} n_i d_i \,, \tag{2}$$

where n is the total number of measurements and n_i the number of measurements corresponding to the grain size d_i.

However, for heterogeneous microstructures it can be argued that the average grain size does not adequately represent the physical response of the material due to the broad grain size dispersion; see e.g. [20,21]. In a microstructure, the largest grains can be associated with low strength due to the length of the slip bands, causing them to yield first; see e.g. [36,37]. Furthermore, even a low number of large grains can occupy a significant material volume. To capture the influence of grain volume, a rule of mixtures approach is proposed for heterogeneous microstructures. The contribution of each grain to the strength of the material is considered to be proportional to the volume of the grain; see e.g. [17,22]. Thus, the volume-weighted average grain size is defined as:

$$d_v = \frac{1}{V_T}\sum_{i=1}^{n} V_i d_i \,, \tag{3}$$

where V_T is the total volume of material and V_i the volume of grains corresponding to the grain size d_i. Because of the different definition, the volume-weighted average grain size is always larger than the average grain size. The two parameters are equal only when all the grains are the same size.

3 Experimental procedures

3.1 Test specimens

To investigate the grain size distribution and its influence on the Hall-Petch relationship, various material microstructures are examined. In addition to structural steel, the weld metals (WM) of conventional arc (CV), laser (LA), and laser-hybrid (HY) welded joints are included in the test series. The weld metals represent complex microstructures with a large variety of grain size distributions. Table 1 lists specimen nomenclature with the corresponding joint type and welding method. Transverse cuts in relation to the welding direction were used for the test specimens. The cut sections were mounted in an electrically conductive resin and grinded using P180-P4000 grit abrasive papers, followed by polishing with 3 µm and 1 µm diamond paste. For optical microscopy and hardness measurements, the specimens were etched with a 2% Nital solution, while polishing with colloidal silica in a vibratory polisher was used as the final step for scanning electron microscopy. The base material (BM) for the welded joints is a shipbuilding structural steel with minimum nominal yield strength of 355 MPa. The steel grades and their properties are listed in Table 2.

Table 1. Test specimen nomenclature and the corresponding joint types and welding methods.

Specimen	Joint type	Welding method	Measurement location
BM.1	Plate, 6 mm	-	1.0-1.9 mm [a]
BM.2	Plate, 5 mm	-	0.75-1.35 mm [a]
CV.1	Butt joint, 3 mm	Arc	Toe, root
CV.2	Block joint, 3 mm	Arc	Toe, root
CV.3	T-joint, 3/5 mm	Arc	Toe
HY.1	Butt joint, 3 mm	Laser-hybrid	Toe, root
LA.1	Butt joint, 3 mm	Laser	Toe
LA.2	Butt joint, 3/5 mm	Laser	Toe

[a]) Distance from the surface of the plate.

Table 2. Mechanical properties and chemical composition of base materials.

		Mechanical properties			Chemical composition											
		Rp0.2	Rm	A	C	Mn	P	S	Si	Al	Cu	Ni	Cr	V	Mo	Fe
Specimen	Grade	(MPa)	(MPa)	(%)	(wt. %)											
BM.1	GL D36	343	472	34	0.11	0.96	0.021	0.007	0.25	0.043	0.03	0.03	0.02	0.002	0.002	Bal.
BM.2	GL D36	400	533	33	0.18	1.39	0.019	0.019	0.24	0.031	0	0.02	0.03	-	0	Bal.
CV.1	S355J2	466	564	31.3	0.169	1.31	0.013	0.012	-	-	0.1	-	-	-	-	Bal.
CV.2	S355J2	466	564	31.3	0.169	1.31	0.013	0.012	-	-	0.1	-	-	-	-	Bal.
CV.3, 3mm	S355J2	466	564	31.3	0.169	1.31	0.013	0.012	-	-	0.1	-	-	-	-	Bal.
CV.3, 5mm	S355J0	432	521	30.3	0.177	0.811	0.023	0.015	0.016	0.032	0.013	0.012	0.018	0	0.001	Bal.
HY.1	GL D36	399	531	26	0.15	1.48	0.013	0.008	0.01	0.037	0.29	0.19	0.06	0	0.01	Bal.
LA.1	GL D36	414	567	24.7	0.1	1.25	-	-	0.002	0.045	0.014	0.014	0.004	0.016	0.031	Bal.
LA.2, 3mm	S355J2	466	564	31.3	0.169	1.31	0.013	0.012	-	-	0.1	-	-	-	-	Bal.
LA.2, 5mm	S355J0	432	521	30.3	0.177	0.811	0.023	0.015	0.016	0.032	0.013	0.012	0.018	0	0.001	Bal.

3.2 Material characterisation

The microstructural quantities and mechanical properties were measured from transverse cross-sections in relation to the welding direction. Example macrosections of the test specimens as well as the toe (t) and root (r) side measurement locations are shown in Figure 1. Because of the narrow weld geometries, instrumented indentation testing was used for measuring the mechanical properties. Hardness was measured with a CSM Instruments micro-indentation tester according to ISO 14577-1 [38] by utilizing a matrix of 10-12 indentations, as shown in Figure 1. Hardness was defined using Martens hardness, denoted by *HM*, with a Vickers pyramid tip and an indentation force of 9.81 N that is large enough to represent the macroscopic hardness of the material; see Appendix A for further details. Linear 30 second loading ramps were used, with a hold time of 10 seconds at the maximum force. The measurements were limited to base material and weld metal to ensure macroscopic homogeneity of the microstructure in the hardness measurement area.

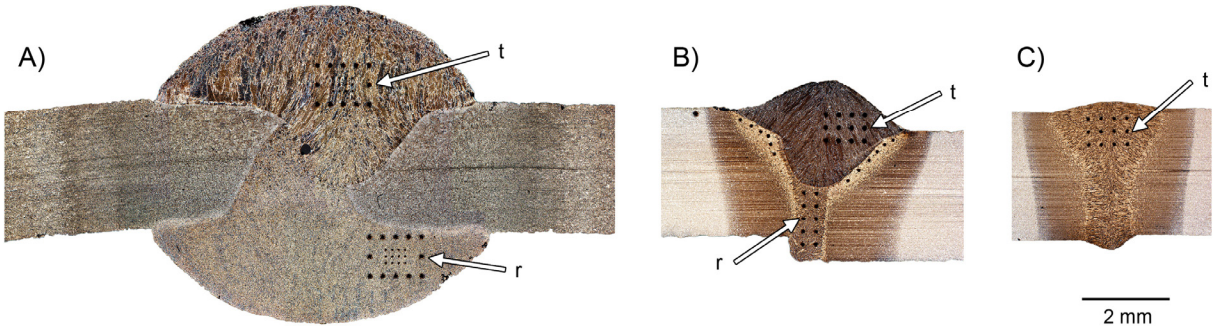

Figure 1. Macrosections of 3 mm butt joints: A) arc welded (CV.1), B) laser-hybrid welded (HY.1), C) laser welded (LA.1).

The microstructures were characterised using electron backscatter diffraction (EBSD) and optical microscopy. EBSD analyses were carried out at the location of hardness indentations or in close proximity where the microstructure is similar; see Figure 2. A Zeiss Ultra 55 field emission scanning electron microscope equipped with a Nordlys F+ camera and Channel 5 software from Oxford Instruments was used for the EBSD analyses. The EBSD analyses were performed with a step size of 0.1 µm at a magnification of 3000x and grain boundary misorientation criteria of 10°. The acceleration voltage was 20 kV and the working distance 19.5 mm. Indexing rate of the EBSD maps varied between 84% and 93% depending on grain size and material phase. On average 90% of the EBSD maps were successfully indexed and a nearest neighbour clean-up routine was used to generate fully indexed maps as recommended by ASTM E2627-10 [39].

In addition to the characterisation of the microstructure with EBSD, the microstructural constituents were identified according to ref. [40]. The volume fractions of microstructural constituents were determined from optical micrographs or EBSD image quality maps using the systematic manual point counting method according to ASTM E562-02 [41]. A randomly placed measurement grid of 100 points was used over 4-6 micrographs to determine the material phase volume fractions.

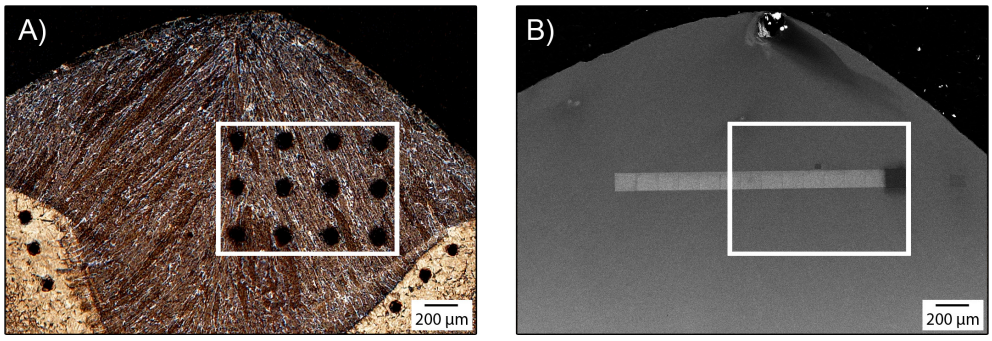

Figure 2. A) Optical micrograph of the hardness measurement area for HY.1 toe weld metal indicated by the white rectangle. B) Placement of EBSD analysis frames shown by the lighter shade of grey.

3.3 Grain size measurement

The grain size distributions were measured from EBSD grain boundary maps and optical micrographs. The images were processed into binary mode, where the grain boundaries are black and the grain interiors are white. The optical micrographs were pre-processed by enhancing the grain boundary delineation and filling holes in the grain interior. The measurement procedures were implemented into the MathWorks MATLAB® software, thus allowing all images to be analysed with the same procedures. Grain size measurements were taken from 2-3 optical micrographs or 4-6 EBSD grain boundary maps depending on the specimen. Prior to grain size measurements the optical micrographs were used to verify that the EBSD analysis images were representative of the microstructure hit by the hardness indentations.

The average grain size was measured using the ASTM E1382 [42] linear intercept length method in four evenly spaced directions (0°, 45°, 90°, 135°). All the measurement directions were considered

as a single distribution for the analysis. Measurements smaller than three pixels, i.e. 0.3 μm for the EBSD grain boundary maps, were considered as noise and removed from the distributions. The distributions measured with the ASTM linear intercept method were characterised with the relative grain size dispersion, modified from Berbenni *et al.* [20]:

$$\frac{\Delta d}{d} = \frac{d_{\max} - d_{\min}}{d} = \frac{P_{99\%} - P_{1\%}}{d}, \tag{5}$$

where the maximum and minimum grain sizes are replaced by the 99% and 1% probability level grain sizes, respectively. This is done to minimise measurement uncertainty, which is inherently at its largest at the extremities of the distribution due to the finite number of measurements.

To determine the volume-weighted average grain size, the point-sampled intercept length method [43,44] was used for measuring the volume-weighted distribution of grain sizes. The method is similar to the ASTM standard method; however, the measurements are carried out at random points. Consequently, different grain sizes are measured proportionally to their surface area fraction. Based on relationships of stereology [45,46] the surface area fraction was used to estimate the volume fraction; see Appendix B for further details. Thus, the average value of the distribution can considered as the volume-weighted average grain size, d_v, as defined in Eq. (3).

The ASTM standard E1382 gives a recommended measurement procedure for the linear intercept length method and it is validated for base material microstructures [42,47]. However, as heterogeneous weld metals can have a large variation in grain size, the recommended measurement procedure was re-evaluated and statistical analysis carried out by varying the number of measurements. The measured grain size converged with decreasing scatter as the number of measurements increased. To accurately capture the tails of the distribution in the experimental data, approximately 20,000-45,000 measurements were made from each image; see Appendix C for further details. The average value converges with 2,000-3,000 measurements for the ASTM linear intercept method and 1500 measurements for the point-sampled intercept length method. These values are higher than the minimum of 500 measurements recommended in ASTM E1382 [42].

4 Results

4.1 Microstructure and grain size distribution

Weld metals have complex microstructures with a large variation in grain size in comparison to base material. The complexity of the weld metal microstructures can be seen from the grain boundary enhanced optical micrographs in Figure 3 and the inverse pole figure (IPF) maps in Figure 4. Furthermore, the weld metals have visibly broader grain size distributions. In addition to the grain size distribution, differences were also found in the microstructural constituents. The base material BM.1 in Figure 3A has a ferritic-pearlitic microstructure with slightly elongated grains and banded pearlite. The microstructural constituents of the CV.1 root-side weld metal in Figure 3B are similar,

although the pearlite is distributed randomly and a small amount of acicular ferrite is present. Most of the weld metals are a mixture of primary ferrite and acicular ferrite, as illustrated by the CV.3 weld metal in Figure 4A. The laser-based welding methods promoted the formation of martensite, as shown in Figure 4B for the LA.1 weld metal. Unlike for the ferritic microstructures, no clear granular structure can be defined for martensite. A characteristic feature of the lath-martensitic microstructure is the presence of low-angle (<10°) boundaries within the 'grains', known as blocks. The blocks, as well as the packets formed by multiple blocks, are separated by high-angle (>10°) boundaries that are shown by the black lines in Figure 4. The martensitic microstructures and the CV.1 toe-side ferritic weld metal were found to have complex grain shapes and thus the transverse cross-section is not representative of the three-dimensional shape of the grains.

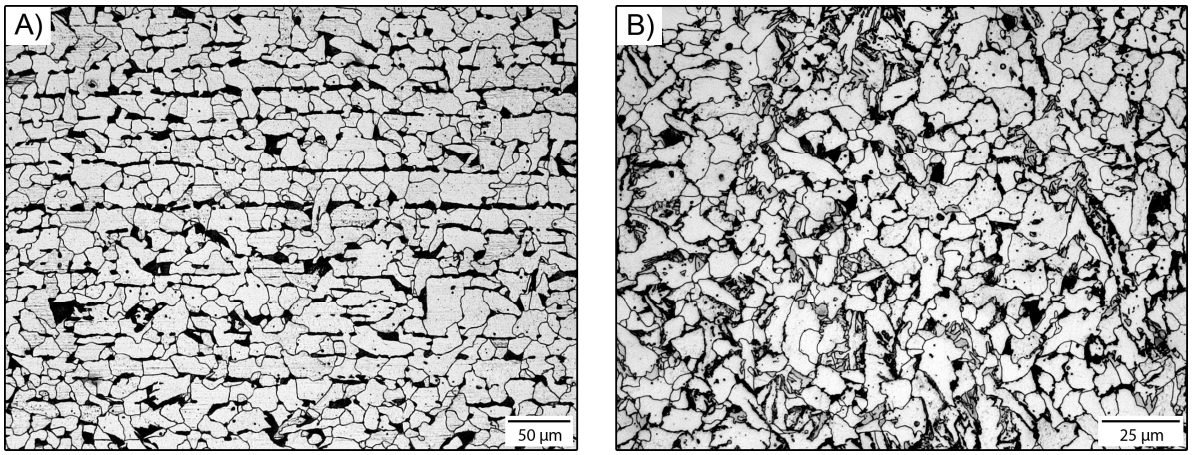

Figure 3. Variety of grain sizes observed in the specimens tested: A) base material BM.1 and B) CV.1 root-side weld metal.

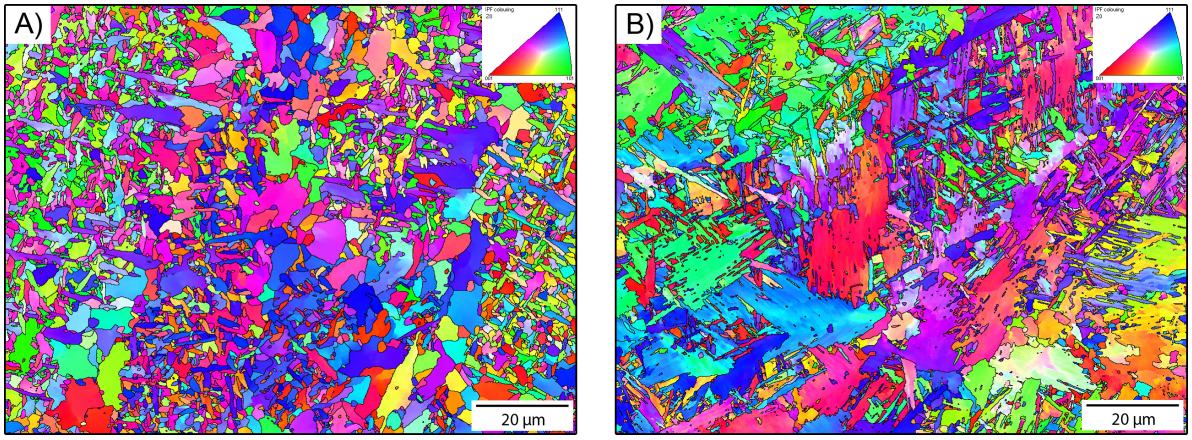

Figure 4. Variety of grain sizes observed in the specimens tested: A) CV.3 and B) LA.1 weld metal. The insert shows the key of the IPF colour map relative to surface normal direction.

To evaluate the applicability of the log-normal distribution used in previous studies, grain size distributions measured with the ASTM linear intercept method are presented in a log-normal probability plot in Figure 5. Significant tail deviations from the log-normal distribution are observed

for most of the specimens. Based on evaluation of other distribution functions, no single distribution function was applicable to all of the measurement data. However, the large data sample can be used directly as the distribution without the need for statistical curve fitting. The dashed lines show the 1% and 99 % probability levels for the characterisation of the distributions according to Eq. (5). Measurement was limited by resolution at the probability level of 1% for the specimens with the smallest average grain sizes; however, the difference from the value predicted by the log-normal fit is negligible when the relative grain size dispersion is considered according to Eq. (5).

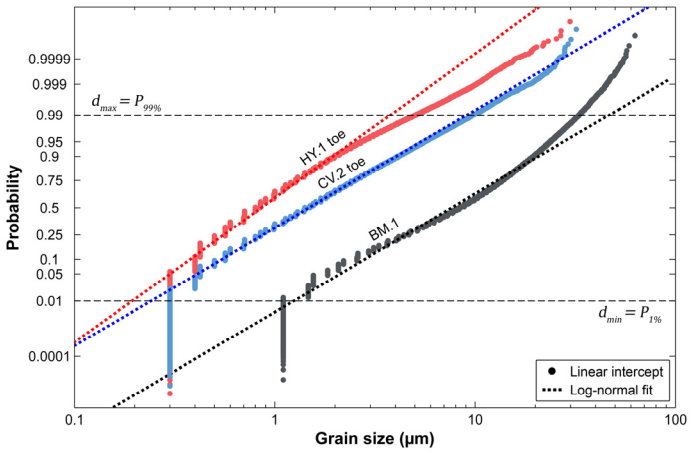

Figure 5. Log-normal probability plot for grain size distributions measured with the ASTM linear intercept method.

To include the influence of grain volume, the point-sampled intercept length method was used for measuring the volume-weighted grain size distributions. A comparison of the grain size distributions measured with the two different methods is presented in Figure 6. For all cases, the influence of small grain sizes is reduced significantly with the volume-weighted method. As a result, the distributions are shifted towards larger grain sizes and the average value, circled in Figure 6, increases. The smallest and largest values of the distributions are equal, but no consistent correlation is observed between the shape of the two distributions.

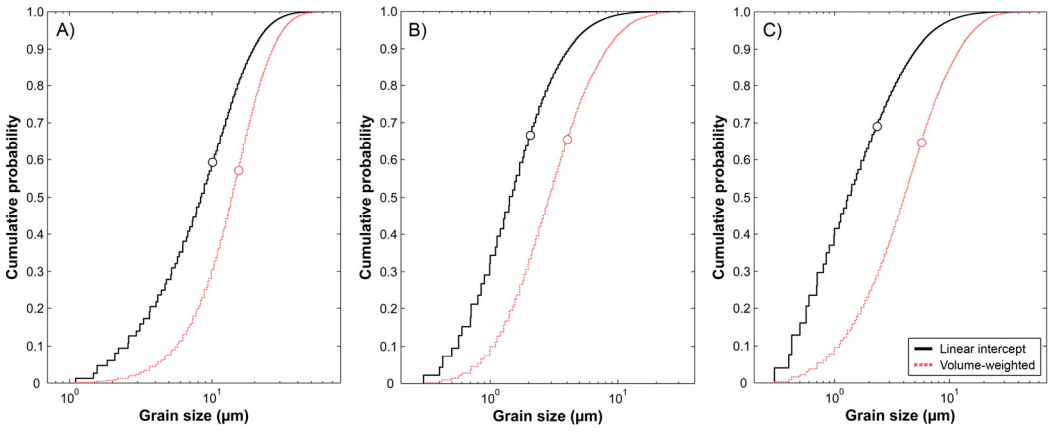

Figure 6. Comparison of cumulative probability distributions for A) base material BM.1, B) CV.2 toe-side weld metal, and C) HY.1 root-side weld metal.

Table 3 summarises the measured average grain sizes, relative grain size dispersions, and hardness values for all test specimens. The volume-weighted average grain size d_v is always larger than the average grain size d and increases of more than 100% are seen for the weld metals. The relative grain size dispersion $\Delta d/d$ is the smallest for the base materials, while the weld metals have a wide range of values.

The microstructural constituent volume fractions and the corresponding 95% confidence intervals are listed in Table 4. Most microstructures have primary ferrite *PF* or acicular ferrite *AF* as their main constituent. The base materials and CV.1 root-side weld metal also have pearlite *P* in their microstructure, while other weld metals have a small amount of ferrite-carbide aggregate *FC* (including pearlite). Laser welds have a martensitic microstructure *M* with a varying amount of ferrite with second phase *FS*. The HY.1 root-side weld metal is a mixture of martensite and ferrite with second phase. According to the microstructural constituents, the specimens are divided into ferritic and martensitic microstructures. The hardness *HM* increases with a decrease in grain size for both ferritic and martensitic microstructures.

Table 3. Measured grain sizes and hardness values and their respective 95 % confidence intervals. ***Error in final published version (specimen name shown as CV.2 root), the error is corrected here.**

Specimen	Images analysed	d (µm)	$\Delta d/d$	d_v (µm)	Increase $d \rightarrow d_v$	Hardness *HM* (MPa)
BM.1	2 (Optical)	9.99 ± 1.62	3.20	15.29 ± 1.96	53 %	1412 ± 29
BM.2	3 (Optical)	4.29 ± 0.20	3.10	6.53 ± 0.39	52 %	1781 ± 53
CV.1 toe	6 (EBSD)	2.90 ± 0.15	5.95	7.28 ± 0.70	151 %	1945 ± 33
CV.1 root*	2 (Optical)	3.53 ± 0.46	3.54	5.95 ± 0.20	69 %	1756 ± 17
CV.2 toe	6 (EBSD)	2.04 ± 0.13	4.66	4.00 ± 0.45	96 %	1984 ± 34
CV.2 root	6 (EBSD)	1.89 ± 0.14	5.38	4.18 ± 0.49	121 %	1931 ± 39
CV.3	4 (EBSD)	1.37 ± 0.08	4.54	2.58 ± 0.21	88 %	2156 ± 29
HY.1 toe	6 (EBSD)	1.09 ± 0.06	4.34	2.06 ± 0.27	89 %	2405 ± 38
HY.1 root	4 (EBSD)	2.30 ± 0.34	5.75	5.64 ± 1.06	145 %	2617 ± 51
LA.1	6 (EBSD)	1.36 ± 0.06	5.42	3.17 ± 0.34	133 %	3339 ± 101
LA.2	6 (EBSD)	1.32 ± 0.08	5.00	2.88 ± 0.24	118 %	3801 ± 46

Table 4. Microstructural constituent volume fractions and the corresponding 95% confidence intervals. Abbreviations used: primary ferrite (PF), acicular ferrite (AF), ferrite with second phase (*FS*), ferrite carbide aggregate (FC), pearlite (*P*), martensite (*M*).

		Constituent volume fraction (%)				
Specimen	Images analysed	*AF*	*PF*	*FS*	*FC / P*	*M*
BM.1	6 (Optical)	-	78.6 ± 5.3	-	21.4 ± 5.3 (P)	-
BM.2	4 (Optical)	-	68.8 ± 5.3	-	31.2 ± 5.3 (P)	-
CV.1 toe	6 (Optical)	34.2 ± 6.1	42.5 ± 2.4	18.8 ± 7.2	4.5 ± 1.2	-
CV.1 root	4 (Optical)	7.3 ± 1.4	78.7 ± 4.7	-	14.0 ± 3.4 (P)	-
CV.2 toe	6 (EBSD)	46.0 ± 3.9	49.5 ± 3.6	-	4.5 ± 1.0	-
CV.2 root	6 (EBSD)	37.5 ± 6.4	56.2 ± 5.3	-	6.3 ± 1.6	-
CV.3	4 (EBSD)	50.3 ± 6.2	45.7 ± 6.6	-	4.0 ± 1.1	-
HY.1 toe	6 (EBSD)	61.2 ± 6.3	32.5 ± 6.6	-	6.3 ± 1.4	-
HY.1 root	6 (Optical)	-	-	54.3 ± 5.6	3.0 ± 0.9	42.7 ± 5.0
LA.1	6 (Optical)	-	-	16.7 ± 2.1	2.0 ± 0.9	81.3 ± 2.3
LA.2	5 (Optical)	-	-	1.4 ± 1.3	1.0 ± 0.8	97.6 ± 1.3

4.2 Correlation of grain size parameters and microstructure

Based on a detailed analysis of the results, the difference between the average grain size and the volume-weighted average grain size is found to be proportional to the relative grain size dispersion; the ratio of the Hall-Petch grain size parameters, i.e. $d^{-1/2}$ and $d_v^{-1/2}$, is plotted as a function of $\Delta d/d$ in Figure 7. The regression analysis is done for individual micrographs, sorted by their microstructural constituents in descending order of volume fraction, with the exception of specimens with acicular ferrite and primary ferrite (*AF, PF*) being shown as a single dataset; see Table 4 for microstructural constituent volume fractions. The regression has narrow 95% confidence and prediction bounds, shown by the dashed and dotted lines, respectively. The correlation between the grain size parameters is:

$$d_v^{-1/2} = d^{-1/2}(c + f\frac{\Delta d}{d}), \tag{6}$$

where f and c are the slope and constant term of the linear regression, respectively. The parameters of the linear regression and their respective 95 % confidence intervals are $f = -0.0635$ (−0.0662, −0.0608) and $c = 1.0059$ (0.9926, 1.0191). Consequently, the constant term is taken to have the value $c \approx 1.0$ in the further analysis of the present study.

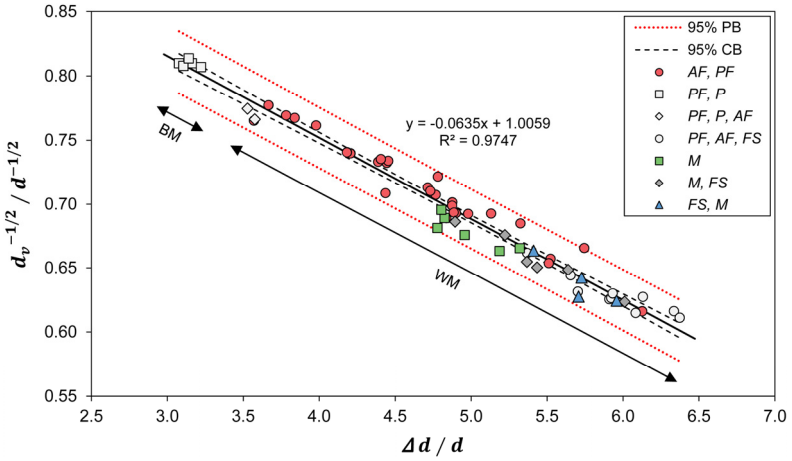

Figure 7. Relation of average d and volume-weighted average d_v grain size as a function of the relative grain size dispersion $\Delta d/d$.

Based on the results in Figure 7, the relative grain size dispersions for base material and weld metal are significantly different. For base material with primary ferrite-pearlite (*PF, P*) microstructure, the relative grain size dispersion is approximately 3.1, while the range for weld metals is 3.5-6.4. Dominantly single phase weld metals, such as martensite (*M*), are grouped within a small range of dispersion. As the volume fraction of ferrite with second phase (*FS*) increases in the martensitic microstructure, the relative grain size dispersion range expands from 4.8-5.3 up to a maximum of 6.0. Likewise, when primary ferrite-pearlite (*PF, P*) has a small addition of acicular ferrite (*AF*), the

dispersion increases from 3.1 to 3.6. Most noticeably, the specimens with acicular ferrite and primary ferrite (*AF, PF*) cover a large range of dispersion ranging from 3.6 to 6.1. To investigate the large range of dispersion, an analysis was carried out to determine the volume fractions of the microstructural constituents from the micrographs. The analysis in Figure 8 shows that the relative grain size dispersion has a linear correlation with the volume fraction of acicular ferrite. With a high volume fraction of acicular ferrite the relative grain size dispersion is narrow, while with a decreasing amount of acicular ferrite the dispersion broadens, as shown in Figure 9.

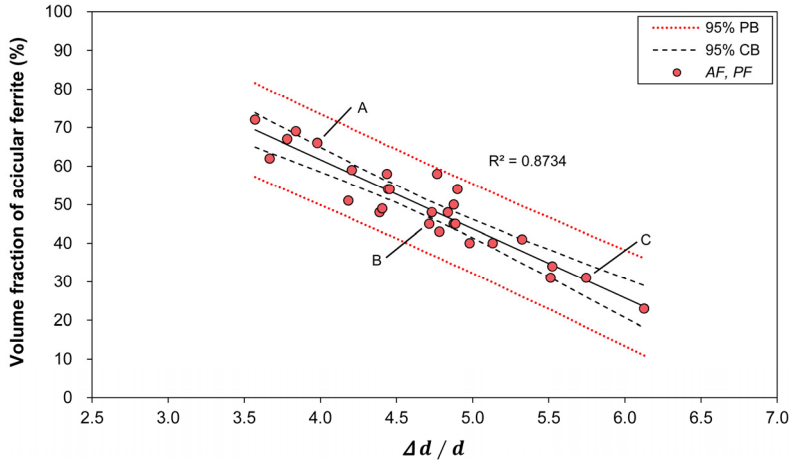

Figure 8. Volume fraction of acicular ferrite as a function of the relative grain size dispersion *Δd/d* for specimens with a mixture of acicular ferrite and primary ferrite.

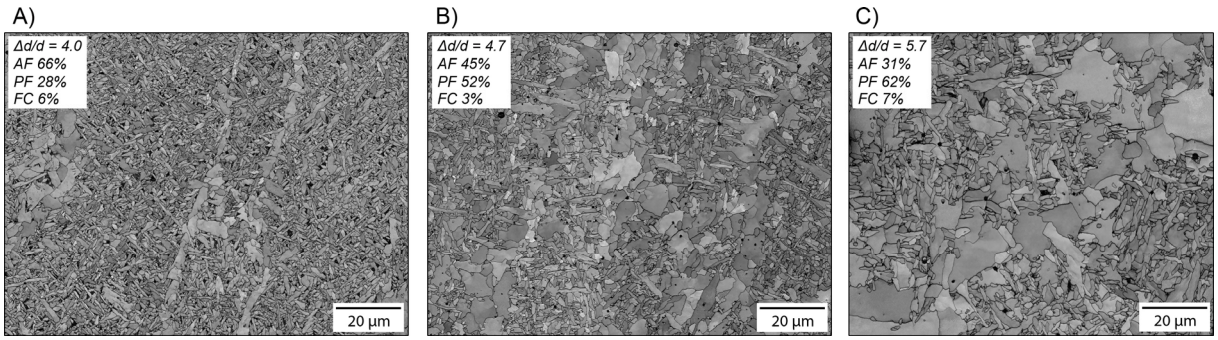

Figure 9. EBSD image quality maps and the microstructural constituents for three different relative grain size dispersions corresponding to Figure 8*: A) Δd/d = 4.0, B) Δd/d = 4.7, C) Δd/d = 5.7.*

4.3 Modified Hall-Petch relationship

To consider the influence of grain size distribution, the volume-weighted average grain size is used in the Hall-Petch relationship. The volume-weighted average grain size can be determined experimentally or through linear regression with Eq. (6). The modified Hall-Petch equation for yield strength is then correspondingly:

$$\sigma = \sigma_0 + kd_v^{-1/2} = \sigma_0 + kd^{-1/2}(1 + f\frac{\Delta d}{d}). \quad (7)$$

The modified Hall-Petch equation is applied to the simulated yield strength of steel from Berbenni *et al*. [20]. The distinct dependence on the grain size distribution is shown in the original results in Figure 10A. As the volume-weighted average grain size is determined using Eq. (7), all grain size distributions are shifted close to the $\Delta d/d = 0$ slope in Figure 10B.

The hardness of ferritic microstructures, excluding the CV.1 toe-side weld metal because of the three-dimensionality of the grain shape, is shown as a function of the average grain size in Figure 10C. Even though the coefficient of determination for the linear regression is high, the 95% confidence and prediction bounds shown by the dashed and dotted lines, respectively, are broad. The bounds are significantly narrower when the volume-weighted average grain size is used in Figure 10D. Furthermore, the coefficient of determination is improved and the data follows the regression within the 95% confidence intervals of the data.

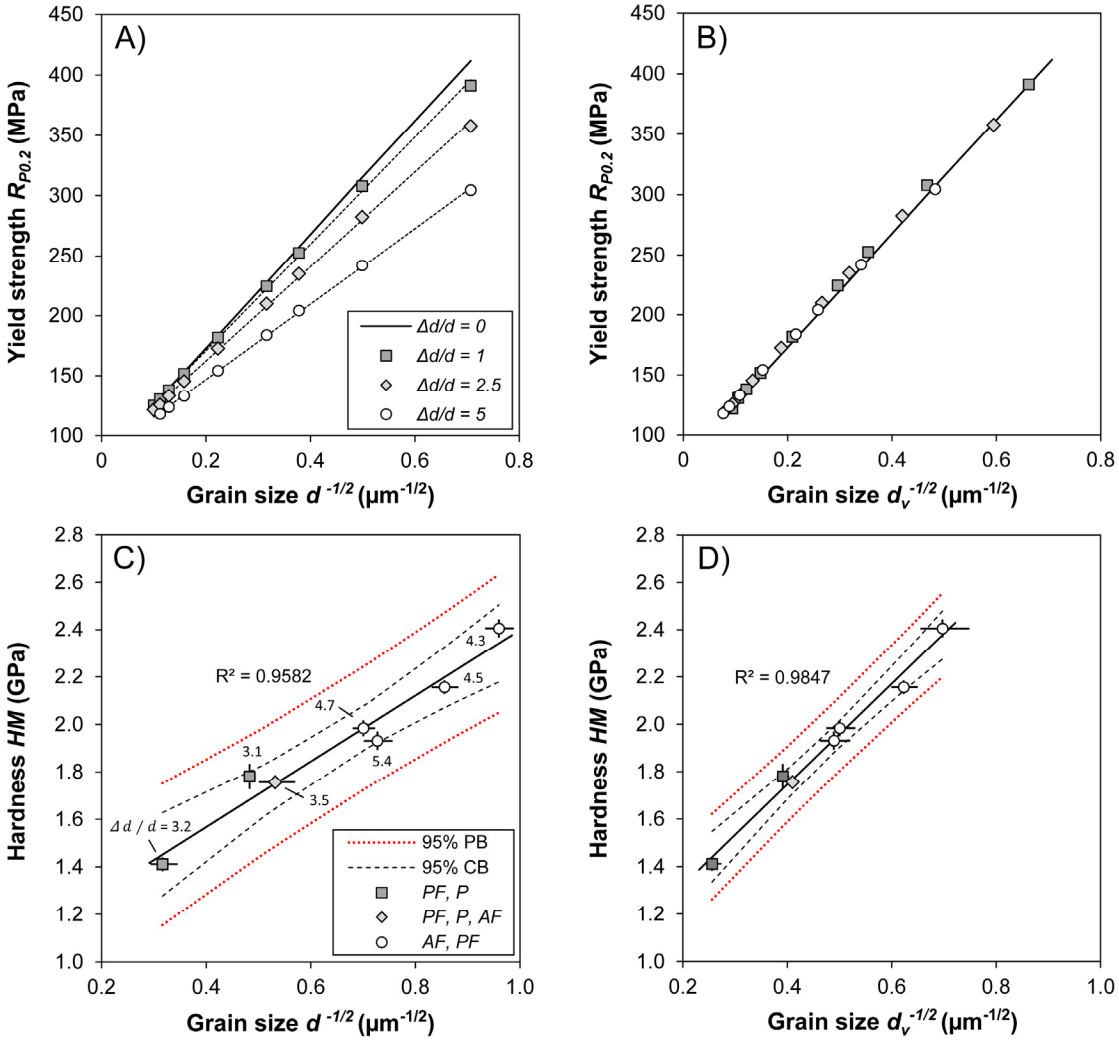

Figure 10. Mechanical response of steel as a function of average *d* and volume-weighted average d_v grain size: A, B) simulated results of Berbenni *et al.* [20], C, D) experimental results for the hardness of ferritic microstructures.

5 Discussion

The grain size distribution and its influence on the mechanical properties of welded structural steel was investigated experimentally. The base materials and weld metals were found to have distinct differences in the complexity of the microstructure and consequently in the grain size distribution. Conventional characterisation methods were compared to the proposed volume-weighted approach and the applicability of different grain size parameters was evaluated based on the Hall-Petch relationship.

The experimentally measured grain size distributions show that the weld metals have a large variety of grain size distributions that are noticeably broader than those of the base material. Thus, the distributions need to be characterised, in addition to the average grain size. Previous numerical studies [16,17,20] have come to the same conclusion for single-phase base materials when different grain

size dispersions are compared. In previous studies [16,20,21,24,27] a large variety of grain size dispersions has been applied to a single phase material. However, in the present study the analysis in Figures 7-9 indicates that the grain size dispersion of weld metal is controlled by the phase contents. This is particularly visible for mixtures of acicular ferrite and primary ferrite that cover a wide range of dispersions. Contrary to the previous studies, the measured grain size distributions have a variety of different distribution shapes that deviate from the log-normal distribution, as shown in Figure 5. Therefore, the parameters of the log-normal distribution are not representative of the grain size distributions and the approach proposed by Raeisinia and Sinclair [23] cannot be used for the investigated base materials and weld metals. However, despite the different distribution shapes, the relative grain size dispersion can be calculated from the measured distributions according to Eq. (5) without statistical curve fitting.

The correlation between the experimentally measured traditional and volume-weighted grain size distributions is not consistent as shown in Figure 6. This can be related to differences in the shape of the grains between the specimens and within a single microstructure. Thus, the assumed shape-similarity of all grains [16,24–27] cannot be used with weld metal microstructures for determining the volume-weighted distribution. However, the volume-weighted average grain size correlates directly with the average grain size and the relative grain size dispersion; see Figure 7. The correlation applies to all microstructures that were examined regardless of material phase, grain shape, or microstructural texture. Thus, the data from traditional grain size measurements can be used for determining the volume-weighted average grain size with good accuracy.

The experimentally measured hardness values in Figure 10C show a trend for the Hall-Petch slope to be dependent on the relative grain size dispersion when the average grain size is used. Therefore, the regression analysis should be performed separately for specific relative grain size dispersions. In previous numerical simulations the Hall-Petch slope has also been found to be dependent on the grain size distribution [16,19–21], as shown in Figure 10A for the results of Berbenni *et al.* [20]. If the modified Hall-Petch relationship (7) is used, the slope is no longer dependent on the grain size distribution for the results of Berbenni *et al.* [20] or the experimentally measured values; see Figure 10B and Figure 10D. The volume fraction of acicular ferrite and primary ferrite does not seem to have a large impact on the Hall-Petch relationship of weld metals, even though they are reported to have different dislocation densities [48,49]. This indicates that the more profound effect arises from the grain size dispersion caused by the phase mixture. The approach presented here is of a general nature and it is not dependent on the distribution function parameters since the 99% and 1% probability level grain sizes are used for the characterisation of the distributions. In addition, the results in Figure 10B are in good agreement with the approach of Raeisinia and Sinclair [23], which is specific to log-normal grain size distribution.

For practical purposes, the original Hall-Petch relationship (1) is applicable when materials with similar grain size distributions and microstructure, e.g. base materials, are compared. The modified relationship (7) is more suitable for ferritic weld metals and heterogeneous microstructures since it

considers the influence of grain size distribution. The results indicate that the volume-weighted average grain size, based on the rule of mixtures, captures the response of the material better than the average grain size as the characteristic length of the microstructure. This finding is supported by earlier investigations, where the rule of mixtures has been successfully applied to model grain boundary behaviour [50], elastic properties of multi-phase materials [51], and strength of composites [52,53].

6 Conclusions

In this paper, the influence of grain size distribution on the Hall-Petch relationship was investigated experimentally for heterogeneous microstructures. Grain size measurements carried out for structural steel weld metals revealed a large variety of grain size distributions that were noticeably broader than those of the base material due to differences in the phase contents. Therefore, the distributions need to be characterised in addition to the average grain size. Because of the large variety of distribution shapes, the parameters of e.g. log-normal distribution could not be used for the characterisation of the distributions. However, the relative grain size dispersion, as defined by the 99% and 1% probability level grain sizes, was found to be a representative parameter of the grain size distribution.

The volume-weighted average grain size, based on a rule of mixtures, was introduced for the determination of the material characteristic length to consider the influence of grain size distribution. The contribution of each grain to the strength of the material was considered to be proportional to the volume of the grain. The volume-weighted average grain size was found to have a strong correlation with the average grain size and relative grain size dispersion obtained from traditional grain size measurements. Thus, the approach can be applied with the use of existing grain size measurement methods.

The experimental results showed that the dependence of the Hall-Petch relationship on the grain size distribution is eliminated when the volume-weighted average grain size is used instead of the average grain size. Therefore, the Hall-Petch relationship was modified by using the volume-weighted average grain size. The modified relationship was found to be applicable to weld metals as well as base materials as all grain size distributions followed a single slope. While the original Hall-Petch relationship is applicable to similar grain size distributions, e.g. base materials, the modified relationship can be used for ferritic weld metals regardless of the grain size distribution. In the present study, the grain size was measured from transverse cross-sections, which are not able to capture the three-dimensional grain shape. Further analysis is required for complex three-dimensional grain shapes, including the martensitic microstructures excluded from the analysis, to validate the modified Hall-Petch relationship for a wider range of material phases, grain shapes and microstructural textures.

7 Acknowledgements

The research is related to “Fatigue of Steel Sandwich Panels” (FASA), a Finnish Academy of Science project under grant agreement n° 261286. The financial support is gratefully appreciated.

Appendix A: Selection of hardness measurement parameters

To ensure that the measured hardness represents the macroscopic hardness of the material, a preliminary study was carried out for the selection of the test parameters, focusing on the influence of indentation size effect [54,55] and indentation size in relation to grain size. The indentation size effect was evaluated using a continuous multi-cycle measurement procedure with the test force ranging from 98.07 mN to 9807 mN. As shown in Figure A-1A, hardness decreases with an increase in indentation depth (and test force). When the results are normalised with 9807 mN test force values in Figure A-1B, a test force of 980.7 mN is determined as a threshold value above which indentation size effect is insignificant. To evaluate indentation size in relation to grain size, a test matrix utilizing test forces 1961.4 mN and 9807 mN was used, as shown in Figure 1A. The scatter of hardness was found significantly lower for 9807 mN, and to be representative of the macroscopic hardness of the material. The ratio between indentation diagonal length and average grain size was approximately 10 for the coarse-grained base material BM.1, and significantly higher for the more heterogeneous weld metals, being in the range of 30-80. Thus, a large population of grains is sampled by each indent, and the average value of 10-12 indents can be considered as a good representation of the macroscopic hardness of the material. Example micrographs of indentation size are shown in Figure A-2, where the indentation diagonal lengths are approximately 115 µm, 95 µm, 85 µm, and 70 µm for A-D, respectively.

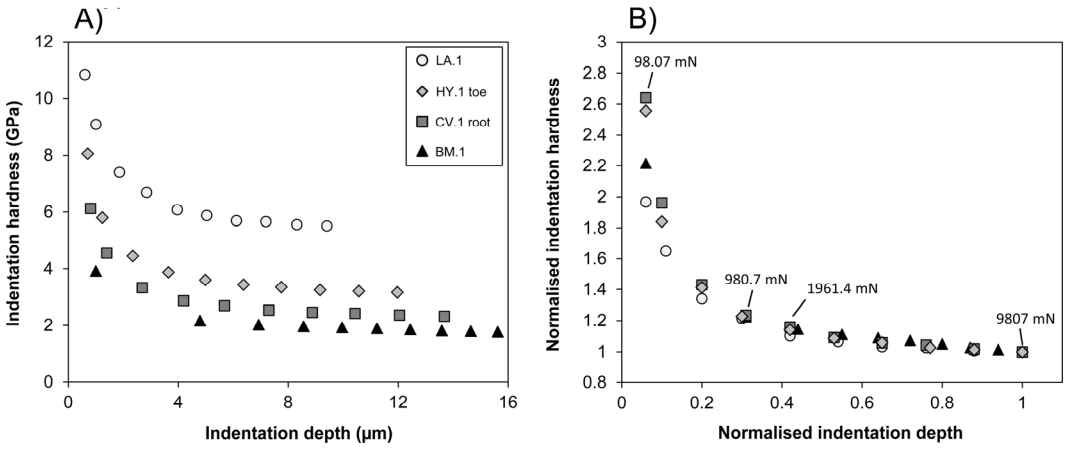

Figure A-1. A) Indentation hardness at varying indentation depth with test forces between 98.07 mN and 9807 mN. B) Indentation hardness and depth normalized with 9807 mN test force values.

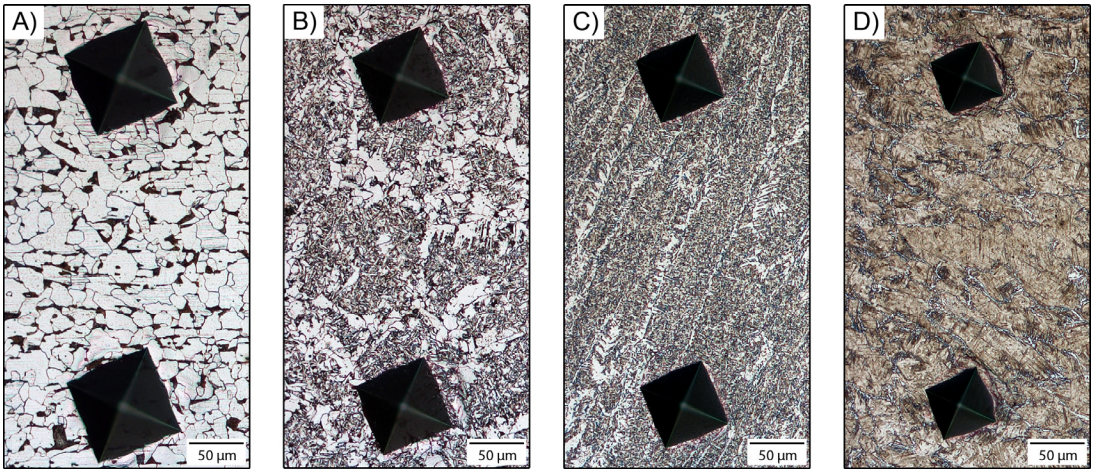

Figure A-2. Indentation size in relation to the grain size for A) base material BM.1 and weld metals of B) CV.2 root-side, C) HY.1 toe-side, and D) LA.1.

Appendix B: Measurement procedure for the volume-weighted average grain size

Obtaining true three-dimensional information of a microstructure is very labour-intensive and has traditionally been done by means of serial sectioning. For this reason, it is common practice to perform three-dimensional estimations from two-dimensional sections. Stereology is the field concerned with indirect methods for estimating three-dimensional features from two-dimensional sections.

The volume-weighted average grain size is obtained by weighting each measurement with the corresponding grain volume, as defined in Eq. (3). This presents the problem of defining the grain volume for each measurement. Although general formulations have been derived for the correlation between intercept length and grain volume [44], it is difficult to determine the accuracy and reliability of such an approach.

The alternative approach is to modify the measurement procedure so that the measured distribution of grain sizes is weighted by grain volume. The point-sampled intercept length method defined by Gundersen and Jensen [43,44] utilises stereological relationships for measuring the volume-weighted distribution of particle size. As described by Kurdyzlowski and Ralph [56], a set of randomly positioned points are placed on the image and an intercept length is measured through each point that hits a location of interest, in this case the interior of the grain. The direction of the intercept is chosen randomly (0°, 45°, 90°, 135°); see Figure B-1 for a graphical illustration of the measurement procedure.

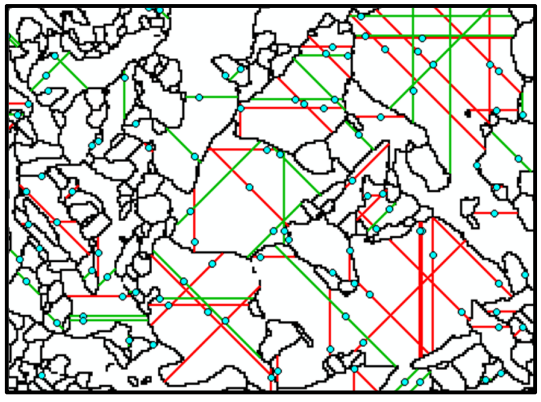

Figure B-1. Measurement of point-sampled intercept length.

The probability of a random point hitting a grain of size i is proportional to the surface area fraction of the grain:

$$P_i = \frac{A_i}{A_T}, \tag{B-1}$$

where A_i is the surface area of a grain of size *i*, and A_T the total surface area. Based on relationships of stereology [45,46] the surface area fraction provides a statistical estimator for the volume fraction:

$$V_V = \frac{V_i}{V_T} = \frac{A_i}{A_T}. \tag{B-2}$$

Equality exists between Eq. (B-1) and Eq. (B-2), and thus the probability of a grain being measured is proportional to its volume fraction. When *n* measurements are taken with the point-sampled method, a distribution is generated where the number of occurrences for a grain of size *i* is determined by the probability of being measured:

$$n_i = nP_i = n\frac{V_i}{V_T}. \tag{B-3}$$

The arithmetic mean grain size for the point-sampled distribution is:

$$\bar{d}_{ps} = \frac{1}{n}\sum_{i=1}^{n} n_i d_i. \tag{B-4}$$

By substituting Eq. (B-3) into Eq. (B-4), the arithmetic mean grain size for the point-sampled distribution is:

$$\bar{d}_{ps} = \frac{1}{n}\sum_{i=1}^{n} n\frac{V_i}{V_T} d_i = \frac{1}{V_T}\sum_{i=1}^{n} V_i d_i, \tag{B-5}$$

which is equal to the volume-weighted average grain size, d_v, as defined in Eq. (3).

Appendix C: Convergence analysis for the grain size measurement

To validate the grain size measurement methods for the characterisation of weld metal, a statistical analysis was carried out by systematically varying the measurement parameters. For the ASTM E1382 [42] linear intercept method, the spacing of the test lines was varied. Analysis for a representative micrograph of two base materials and five weld metals is shown in Figure C-1A as a function of test line spacing. As the test line spacing is reduced, the measured average grain sizes converge towards the value obtained with one pixel spacing. A spacing of seven pixels yields ca. 20,000-45,000 measurements depending on the microstructure, which is well within the ±2.5% bounds as shown in Figure C-1B. The densely spaced test lines are required to accurately capture the tails of the distributions and thus eliminate the need for statistical curve fitting, particularly for weld metals as shown Figure C-2. The micrographs analysed in Figure C-2 correspond to Figure 3A (BM.1) and Figure 4B (LA.1).

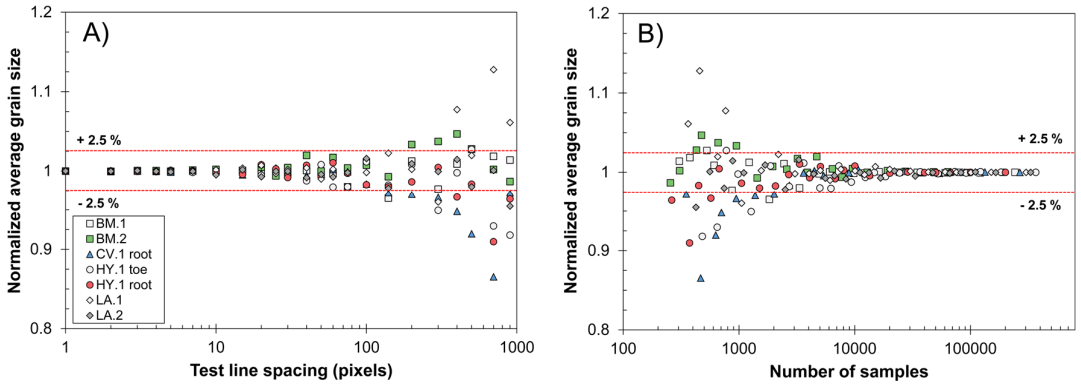

Figure C-1. Influence of A) test line spacing and B) number of samples on the scatter of average grain size for the ASTM linear intercept method.

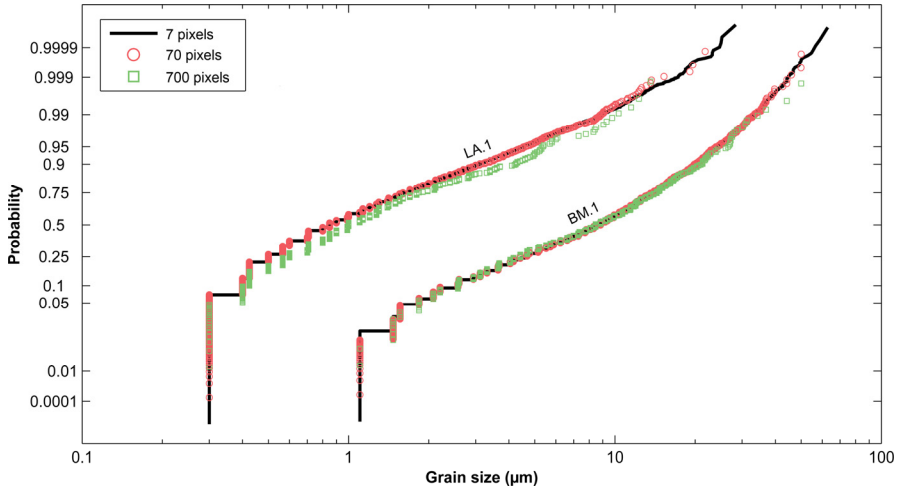

Figure C-2. Log-normal probability plot for base material BM.1 and weld metal LA.1 for different test line spacing values.

The point-sampled intercept length method was validated by varying the number of test points. The validation is performed for two microstructures: base material BM.1 with a relatively narrow grain size distribution (*Δd/d = 3.2)* and LA.1 weld metal with a large variation in grain size (*Δd/d = 6.0)*. The micrographs analysed are shown in Figure 3A (BM.1) and Figure 4B (LA.1). The variation of the volume-weighted average grain size is presented in Figure C-3, which shows the average value and standard deviation of five separate measurements for a single micrograph. Base material BM.1 converges with a low number of test points, while the LA.1 weld metal requires approximately 1500 test points to converge. To accurately capture the distribution tails, 25,000 test points are used for the experiments. Consequently, the value is in the range of measurements taken by the ASTM linear intercept method (20,000-45,000). As convergence was observed for the two extreme cases, it was assumed that all other specimens converge as well.

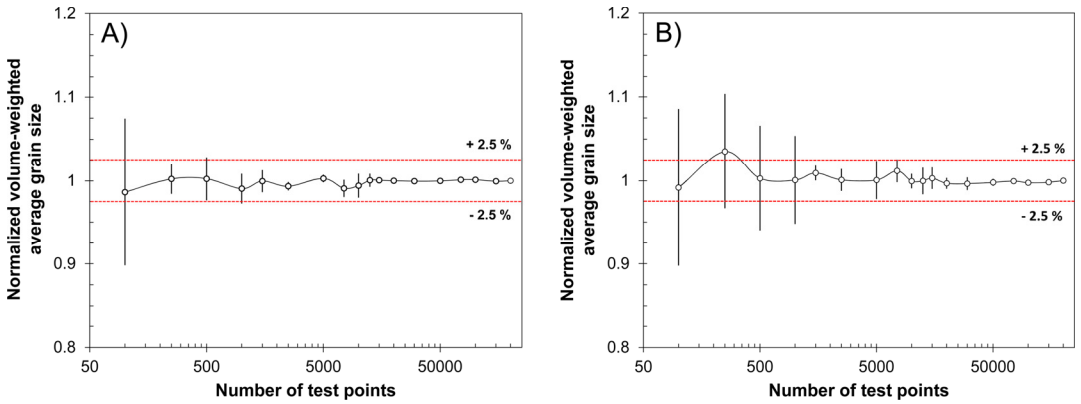

Figure C-3. Influence of number of test points on the volume-weighted average grain size for A) base material BM.1 and B) LA.1 weld metal.

References

[1] D. Boronski, Int. J. Fatigue 28 (2006) 346.

[2] M. Gao, X. Zeng, J. Yan, Q. Hu, Appl. Surf. Sci. 254 (2008) 5715.

[3] M. Gao, X. Zeng, Q. Hu, J. Yan, J. Mater. Process. Technol. 209 (2009) 785.

[4] M. Sokolov, A. Salminen, M. Kuznetsov, I. Tsibulskiy, Mater. Des. 32 (2011) 5127.

[5] H. Remes, Int. J. Fatigue 52 (2013) 114.

[6] E.O. Hall, Proc. Phys. Soc. B.64 (1951) 747.

[7] N.J. Petch, J. Iron Steel Inst. 174 (1953) 25.

[8] R.A. Masumura, P.M. Hazzledine, C.S. Pande, Acta Mater. 46 (1998) 4527.

[9] E.O. Hall, Nature 173 (1954) 948.

[10] R.W. Armstrong, I. Codd, R.M. Douthwaite, N.J. Petch, Philos. Mag. 7 (1962) 45.

[11] R.W. Armstrong, Metall. Mater. Trans. 1 (1970) 1169.

[12] S. Tachibana, S. Kawachi, K. Yamada, T. Kunio, Nippon Kikai Gakkai Ronbunshu, A Hen/Transactions Japan Soc. Mech. Eng. Part A 54 (1988) 1956.

[13] M. Furukawa, Z. Horita, M. Nemoto, R.Z. Valiev, T.G. Langdon, Acta Mater. 44 (1996) 4619.

[14] M.. Chapetti, H. Miyata, T. Tagawa, T. Miyata, M. Fujioka, Mater. Sci. Eng. A 381 (2004) 331.

[15] N. Hansen, Scr. Mater. 51 (2004) 801.

[16] S. Ramtani, H.Q. Bui, G. Dirras, Int. J. Eng. Sci. 47 (2009) 537.

[17] K.J. Kurzydlowski, J.J. Bucki, Acta Metall. Mater. 41 (1993) 3141.

[18] J.R. Weertman, P.G. Sanders, C.J. Youngdahl, Mater. Sci. Eng. A 234-236 (1997) 77.

[19] T. Morita, R. Mitra, J.R. Weertman, Mater. Trans. 45 (2004) 502.

[20] S. Berbenni, V. Favier, M. Berveiller, Comput. Mater. Sci. 39 (2007) 96.

[21] B. Raeisinia, C.W. Sinclair, W.J. Poole, C.N. Tomé, Model. Simul. Mater. Sci. Eng. 16 (2008) 025001.

[22] K.J. Kurzydlowski, Scr. Metall. Mater. 24 (1990) 879.

[23] B. Raeisinia, C.W. Sinclair, Mater. Sci. Eng. A 525 (2009) 78.

[24] B. Zhu, R.J. Asaro, P. Krysl, R. Bailey, Acta Mater. 53 (2005) 4825.

[25] B. Zhu, R.J. Asaro, P. Krysl, K. Zhang, J. Weertman, Acta Mater. 54 (2006) 3307.

[26] M.P. Phaniraj, M.J.N.V. Prasad, A.H. Chokshi, Mater. Sci. Eng. A 463 (2007) 231.

[27] Y. Liu, J. Zhou, X. Ling, Mater. Sci. Eng. A 527 (2010) 1719.

[28] J.C.M. Li, Trans. Met. Soc. AIME 227 (1963) 239.

[29] H. Conrad, Acta Metall. 11 (1963) 75.

[30] K.-H. Chia, K. Jung, H. Conrad, Mater. Sci. Eng. A 409 (2005) 32.

[31] M.F. Ashby, Philos. Mag. 21 (1970) 399.

[32] U.F. Kocks, Metall. Trans. 1 (1970) 1121.

[33] A.W. Thompson, M.I. Baskes, W.F. Flanagan, Acta Metall. 21 (1973) 1017.

[34] T.T. Zhu, A.J. Bushby, D.J. Dunstan, Mater. Technol. 23 (2008) 193.

[35] L.P. Evers, D.M. Parks, W. a. M. Brekelmans, M.G.D. Geers, J. Mech. Phys. Solids 50 (2002) 2403.

[36] S. Takaki, Mater. Sci. Forum 654-656 (2010) 11.

[37] B. Raeisinia, W.J. Poole, Model. Simul. Mater. Sci. Eng. 20 (2012) 015015.

[38] ISO 14577-1:2002, Metallic Materials. Instrumented Indentation Test for Hardness and Materials Parameters. Part 1: Test Method, International Organization for Standardization, Geneva, 2002.

[39] ASTM E 2627 - 10, Standard Practice for Determining Average Grain Size Using Electron Backscatter Diffraction (EBSD) in Fully Recrystallized Polycrystalline Materials, ASTM International, West Conshohocken, PA, 2010.

[40] Weld. World 29 (1991) 160.

[41] ASTM E 562 – 02, Standard Test Method for Determining Volume Fraction by Systematic Manual Point Count, ASTM International, West Conshohocken, PA, 2002.

[42] ASTM E1382 - 97 (2004), Standard Test Methods for Determining Average Grain Size Using Semiautomatic and Automatic Image Analysis, ASTM International, West Conshohocken, PA, 2004.

[43] H.J.G. Gundersen, E.B. Jensen, J. Microsc. 131 (1983) 291.

[44] H.J.G. Gundersen, E.B. Jensen, J. Microsc. 138 (1985) 127.

[45] E.E. Underwood, Quantitative Stereology, Addison-Wesley Publishing Co., Reading, MA, 1970.

[46] ASTM E1245 - 03, Standard Practice for Determining the Inclusion or Second-Phase Constituent Content of Metals by Automatic Image Analysis, ASTM International, West Conshohocken, PA, 2003.

[47] ASTM E112 - 96 (2004), Standard Test Methods for Determining Average Grain Size, ASTM International, West Conshohocken, PA, 2004.

[48] J.R. Yang, H.K.D.H. Bhadeshia, Am. Weld. J. 69 (1990) 305.

[49] H.K.D.H. Bhadeshia, Bainite in Steels, 2nd ed., IOM Communications LTD, London, 2001.

[50] H.S. Kim, Y. Estrin, M.B. Bush, Acta Mater. 48 (2000) 493.

[51] Y. Prawoto, J.R.P. Djuansjah, N.B. Shaffiar, Comput. Mater. Sci. 65 (2012) 528.

[52] H.S. Kim, S.I. Hong, S.J. Kim, J. Mater. Process. Technol. 112 (2001) 109.

[53] Y. Hu, T. Nakao, T. Nakai, J. Gu, F. Wang, J. Wood Sci. 51 (2005) 7.

[54] W.D. Nix, H. Gao, J. Mech. Phys. Solids 46 (1998) 411.

[55] R. Rodriguez, I. Gutierrez, Mater. Sci. Eng. A 361 (2003) 377.

[56] K.J. Kurzydlowski, B. Ralph, The Quantitative Description of the Microstructure of Materials, CRC Press LLC, Boca Raton, Florida, 1995.